Delayed synchronization of activity in cortex and subthalamic nucleus following cortical stimulation in the rat

Peter J. Magill[1], Andrew Sharott[2], J. Paul Bolam[1] and Peter Brown[2]

[1] *Medical Research Council Anatomical Neuropharmacology Unit, University of Oxford, Oxford, UK*
[2] *Sobell Department of Motor Neuroscience and Movement Disorders, Institute of Neurology, London, UK*

Oscillations may play a role in the functional organization of cortico-basal ganglia-thalamocortical circuits, and it is important to understand their underlying mechanisms. The cortex often drives basal ganglia (BG) activity, and particularly, oscillatory activity in the subthalamic nucleus (STN). However, the STN may also indirectly influence cortex. The aim of this study was to characterize the delayed (>200 ms) responses of STN neurons to synchronized cortical inputs, focusing on their relationship with oscillatory cortical activity. We recorded the short-latency and delayed responses of STN units and frontal electrocorticogram (ECoG) to cortical stimulation in anaesthetized rats. Similar to previous studies, stimulation of ipsilateral frontal cortex, but not temporal cortex, evoked a short-latency triphasic response, followed by a sustained reduction or pause in firing, in rostral STN units. Caudal STN units did not show the short-latency triphasic response but often displayed a prolonged firing reduction. Oscillations in STN unit activity and ECoG were common after this sustained firing reduction, particularly between 200 and 600 ms after frontal cortical stimulation. These delayed oscillations were significantly coherent in a broad frequency band of 5–30 Hz. Coherence with ECoG at 5–15 Hz was observed throughout STN, though coherence at 15–30 Hz was largely restricted to rostral STN. Furthermore, oscillatory responses at 5–30 Hz in rostral STN predominantly led those in cortex (mean latency of 29 ms) after frontal cortical stimulation. These findings suggest that STN neurons responding to corticosubthalamic inputs may provide a delayed input to cortex, via BG output nuclei, and thence, thalamocortical pathways.

(Resubmitted 29 March 2006; accepted after revision 12 May 2006; first published online 18 May 2006)
Corresponding author P. J. Magill: Medical Research Council Anatomical Neuropharmacology Unit, University of Oxford, Mansfield Road, Oxford OX1 3TH, UK. Email: peter.magill@pharm.ox.ac.uk

A better understanding of the nature of the functional coupling between neuronal assemblies in the cerebral cortex and basal ganglia (BG) is necessary to fully appreciate the functional organization of the BG. It has been suggested that the synchronization of neuronal activity at relatively high frequencies (i.e. above ∼10 Hz) may be mechanistically important for information processing across different levels of the sensory and motor systems (MacKay, 1997; Engel & Singer, 2001; Engel *et al.* 2001; Buzsáki & Draguhn, 2004). Several studies have shown that oscillatory activity in the cortex and BG may be temporally coupled (Boraud *et al.* 2005). However, although the temporal coupling of oscillations suggests a synchronization of activity in cortex and BG, it provides little insight into the nature of any transformation of information that might be achieved, and whether synchronization *per se* is an integral part of this transformation, as has been suggested in the visual cortex (Singer, 1999).

The observations that deranged synchronization in cortex and BG is common in disorders with prominent motor dysfunction, such as Parkinson's disease (PD) and its animal models (Bergman *et al.* 1998; Levy *et al.* 2000, 2001, 2002; Brown *et al.* 2001; Bevan *et al.* 2002*b*; Boraud *et al.* 2005; Sharott *et al.* 2005*b*; Fogelson *et al.* 2006), and that synchronization varies in a task-dependent fashion (Cassidy *et al.* 2002; Williams *et al.* 2003; Kühn *et al.* 2004), provide circumstantial evidence linking synchronization of activity within cortico-basal ganglia-thalamocortical circuits to information processing. One of the major patterns of synchronization in PD, that in the beta-frequency (15–30 Hz) band, is driven from cortex, at least in the parkinsonian state at rest (Marsden *et al.* 2001;

 DOI: 10.1113/jphysiol.2006.110379

Williams *et al.* 2002; Fogelson *et al.* 2006). As such, an alternative interpretation is that the temporal coupling of cortical and BG activity is an epiphenomenon of cortical synchronization in the same frequency range, similar to the manifestation of the beta rhythm in motor unit discharges that probably arises simply as the product of cortico-spinal connectivity (Brown, 2000). Moreover, the temporal coupling of activity that is evident in BG local field potentials and cortical electroencephalogram recorded in PD patients must involve synchronization across large assemblies of neurons in both BG and cortex (Brown, 2003; Fogelson *et al.* 2006), and is therefore unlikely to contain signals related to specific channels of information processing. Nevertheless, some synchronization of neuronal activity does occur, particularly in the beta-frequency band, in the BG of nonparkinsonian animals and humans, raising the possibility that these oscillations are linked to information processing under physiological rather than pathological conditions (Courtemanche *et al.* 2003; Sochurkova & Rektor, 2003; Berke *et al.* 2004; Magill *et al.* 2004*b*; Sharott *et al.* 2005*a*). If relevant for cortico-basal ganglia-thalamocortical function, one might expect patterns of synchronization to change according to local input, thereby retaining information specific to connectivity, and that, when appropriate, the basal ganglia would lead cortical activity rather than be driven by cortex.

One way to address this issue is to examine the effects of brief cortical stimulation on the relative timing (i.e. phase relationships) and topography of temporally coupled oscillations in subthalamic nucleus (STN) and cortex. Studies employing electrical stimulation of cortex have provided valuable insight into the integration of corticosubthalamic and corticostriatal inputs in the BG (Kita, 1994; Nambu *et al.* 2002). Stimulation of ipsilateral frontal and prefrontal cortices often leads to a short-latency multiphasic response in STN neurons, which is initiated by excitation that is driven by the corticosubthalamic pathway (Kitai & Deniau, 1981; Ryan & Clark, 1992; Fujimoto & Kita, 1993; Maurice *et al.* 1998; Nambu *et al.* 2000; Kolomiets *et al.* 2001; Magill *et al.* 2004*a*). The first three phases of the response, which evolve rapidly (within 50 ms), are usually followed by a sustained reduction in firing of ∼200 ms in duration, which has been proposed to be due to 'disfacilitation' of cortical inputs (Fujimoto & Kita, 1993; Nambu *et al.* 2000). The characteristics and functional relevance of the delayed activity that inevitably marks the end of this prolonged reduction in firing are yet to be determined. As such, it is important to determine whether the delayed responses of STN neurons contain oscillatory components that are related to ongoing rhythmic activity in cortex, or how any such relationship is in turn governed by the topography of the underlying circuits.

To address these issues and further elucidate the temporal coupling of oscillatory activity in STN and cortex, we compared the delayed (>200 ms) responses of STN units and cortical population activity, as recorded in the frontal electrocorticogram (ECoG), to cortical stimulation in anaesthetized rats. Delayed responses were analysed in the frequency domain and activity relationships were defined in terms of coherence and phase (Halliday *et al.* 1995). The dependence of activity relationships on topography was characterized by recording unit activity along the rostrocaudal axis of STN (Magill *et al.* 2004*a*), and by varying the stimulation site between (sensorimotor) frontal cortex, which is known to project directly to STN, and (auditory) temporal cortex, which does not contribute to the corticosubthalamic pathways (Canteras *et al.* 1990; Kolomiets *et al.* 2001).

Methods

Electrophysiological recordings and labelling of recording sites

Experimental procedures were carried out on adult male Sprague-Dawley rats (Charles River, Margate, UK) and were conducted in accordance with the UK Animals (Scientific Procedures) Act 1986.

Electrophysiological recordings were made in seven rats (230–350 g). Anaesthesia was induced with isoflurane (Isoflo; Schering-Plough Ltd, Welwyn Garden City, UK) and maintained with urethane (1.3 g kg^{-1} I.P., ethyl carbamate; Sigma, Poole, UK), and supplemental doses of ketamine (30 mg kg^{-1} I.P., Ketaset; Willows Francis, Crawley, UK) and xylazine (3 mg kg^{-1} I.P., Rompun; Bayer, Germany), as previously described (Magill *et al.* 2001). All wound margins were infiltrated with the local anaesthetic bupivacaine (0.75% w/v; Astra, Kings Langley, UK), and corneal dehydration was prevented with application of Hypromellose eye drops (Norton Pharmaceuticals Ltd, Harlow, UK). Animals were then placed in a stereotaxic frame. Body temperature was maintained at 37 ± 0.5°C with the use of a homeothermic heating device (Harvard Apparatus Ltd, Edenbridge, UK). Anaesthesia levels were assessed by testing reflexes to a cutaneous pinch or gentle corneal stimulation, and by examination of the frontal ECoG (see following text). In terms of using the ECoG to ascertain anaesthesia levels, the expression levels of a slow oscillation at ∼1 Hz and spindle oscillations at ∼10 Hz, which together constitute the major components of the slow-wave activity in this preparation (see Magill *et al.* 2004*b*), were assessed online; deeper anaesthesia is accompanied by higher levels of slow-wave activity. Electrocardiographic (ECG) activity and respiration rate were also monitored constantly to ensure the animals' well being (see following text). Mineral oil or saline solution (0.9% w/v NaCl) was applied to all areas of exposed cortex to prevent dehydration.

Parallel bipolar stimulating electrodes (constructed from nylon-coated stainless steel wires; California Fine Wire, Grover City, CA, USA), with tip diameters of ~100 μm, a tip separation of ~150 μm, and an impedance of ~10 kΩ, were implanted into the right frontal cortex and right temporal cortex, and then affixed to the skull with dental acrylic cement (Associated Dental Products Ltd, Swindon, UK). The coordinates of the frontal stimulation site (AP, +4.2 mm; ML, 3.5 mm (bregma reference); and a depth of 2.3 mm below the dura; Paxinos & Watson, 1986) correspond to the border region between the lateral and medial agranular fields of the somatic sensorimotor cortex (Donoghue & Wise, 1982; Donoghue & Parham, 1983). The coordinates of the temporal stimulation site (AP, −5.2 mm; ML, 6.9 mm; and a depth of 2.3 mm below the dura) approximately correspond to the primary auditory cortex (see Kolomiets *et al.* 2001).

The ECoG was recorded via a 1 mm diameter steel screw juxtaposed to the dura mater above the right frontal cortex (AP, +4.5 mm; ML, 2.0 mm; which corresponds to the medial agranular field of the somatic sensorimotor cortex; Donoghue & Wise, 1982) and referenced against an indifferent electrode placed adjacent to the temporal musculature. This and adjacent regions of cortex project to both striatum and STN, as demonstrated in anatomical and electrophysiological studies (Fujimoto & Kita, 1993; Smith *et al.* 1998; Kolomiets *et al.* 2001; Magill *et al.* 2004*a*), and, thus, activity in these regions is of direct functional relevance. Raw ECoG was band-pass filtered (0.1–2000 Hz, −3 dB limits) and amplified (×2000, NL104 preamplifier; Digitimer Ltd, Welwyn Garden City, UK) before acquisition. The ECG was differentially recorded via two silver wires that were inserted subcutaneously into the ipsilateral forelimb and hindlimb. Raw ECG was band-pass filtered (10–100 Hz) and amplified (×5000, NL104; Digitimer) before acquisition. The chest movements accompanying respiration were recorded using a miniature accelerometer (AP19; Bay Systems Ltd, Somerset, UK) and charge amplifier (Type 5007; Kistler Instrumente AG, Winterthur, Switzerland). The signal from the accelerometer allowed the depth and rate of respiration to be accurately assessed on- and off-line (Magill *et al.* 2004*b*).

Extracellular recordings of action potentials in the ipsilateral STN were made with glass electrodes (6–12 MΩ measured at 10 Hz *in situ*, tip diameters of 2.0–3.0 μm) that were filled with a 0.5 M NaCl solution containing 1.5% w/v Neurobiotin (Vector Laboratories, Peterborough, UK). Electrodes were lowered into the brain using a computer-controlled stepper motor (Burleigh IW-711; Scientifica Ltd, Harpenden, UK), which allowed the electrode depth to be determined with a resolution of 0.5 μm. Extracellular signals from the electrode were amplified (×10) through the active bridge circuit of an Axoprobe 1A amplifier (Axon Instruments, Union City, CA, USA), AC-coupled and amplified a further ×100 (NL106; Digitimer), before band-pass filtering (between 0.4 and 4 kHz; NL125, Digitimer). Signals were digitized on-line (see below) and simultaneously displayed on an oscilloscope (DSO 610; Gould Instruments, Ilford, Essex, UK). Action potentials were typically between 0.4 and 1.2 mV in amplitude and always exhibited an initial positive deflection (Magill *et al.* 2000, 2001).

The responses of STN neurons to cortical inputs were determined by focal electrical stimulation of the cortex (Maurice *et al.* 1998; Kolomiets *et al.* 2001; Magill *et al.* 2004*a*). Note that the first three phases of the short-latency responses to cortical stimulation have been previously reported in the same animals (Magill *et al.* 2004*a*). Electrical stimuli, which consisted of single square-wave current pulses of 0.3 ms duration and variable amplitude (300–600 μA to ensure maximal responses; see Magill *et al.* 2004*a*), were delivered to the ipsilateral frontal or temporal cortices at a frequency of 0.67 Hz using a constant current isolator (A360D; World Precision Instruments Ltd, Stevenage, UK) that was gated by a programmable pulse generator (Master-8; AMPI, Jerusalem, Israel). Between 210 and 230 cortical stimuli were delivered for each STN neuron tested. Stimulation of frontal cortex at this and similar frequencies (0.4–1.4 Hz) evokes robust and stable single-cell and population responses in STN (Maurice *et al.* 1998; Nambu *et al.* 2000; Kolomiets *et al.* 2001; Magill *et al.* 2004*a*). However, we cannot rule out the possibility that stimulation at 0.67 Hz may have induced synaptic plasticity in the cortex and/or STN (or related neural circuits), and thus, it would be of interest to test in the future whether the responses described hereafter vary with stimulation parameters.

Between two and five electrode tracks were performed in each animal. The final recording location in each experiment was marked by a discrete extracellular deposit of Neurobiotin (100 nA anodal current; 1 s (50%) duty cycle for 60 min; Magill *et al.* 2004*b*). Following a period of 1–2 h for the uptake and transport of the Neurobiotin by neurons and glia at the recording site, animals were given a lethal dose of ketamine anaesthetic (200 mg kg^{-1}, I.P.) and perfused via the ascending aorta with 100 ml of 0.01 M phosphate-buffered saline (PBS) at pH 7.4, followed by 300 ml of 4% w/v paraformaldehyde and 0.1% w/v glutaraldehyde in 0.1 M phosphate buffer, pH 7.4, and then by 150 ml of the same solution without glutaraldehyde. Brains were then postfixed in the latter solution at 4°C for at least 12 h before sectioning.

Histochemistry

Standard techniques were used to visualize the Neurobiotin deposits (see Magill *et al.* 2001). Briefly, the fixed brain was cut into 60 μm thick sections in the coronal

plane on a vibrating blade microtome (VT1000S; Leica Microsystems, Milton Keynes, UK). Sections were washed in PBS and incubated overnight in avidin-biotin-peroxidase complex (1:100; Vector) in PBS containing 0.2% v/v Triton X-100 and 1% w/v bovine serum albumin (Sigma). After washing, the sections were incubated in hydrogen peroxide (0.002% w/v; Sigma) and diaminobenzidine tetrahydrochloride (0.025% w/v; Sigma) in the presence of nickel ammonium sulphate (0.5% w/v; Sigma) dissolved in Tris buffer (0.05 M, pH 8.0) for 15–30 min. Neurobiotin-filled cells were intensely labelled with an insoluble, black/blue precipitate (Fig. 1*A* and *B*; see also Magill *et al.* 2004*b*). Finally, sections were dehydrated, cleared and mounted for light microscopy using standard techniques (Bolam, 1992).

All final recording sites and the locations of the stimulation electrodes were histologically verified (Fig. 1*A* and *B*). An STN neuron was defined as 'rostral' or 'caudal' when it was clearly located within either the rostral half of STN (approximately between 3.3 and 3.8 mm posterior of bregma; see Paxinos & Watson, 1986) or caudal half of the STN (approximately between 3.9 and 4.3 mm posterior of bregma), respectively, as determined by histological examination of the STN in which it was recorded. The locations of all STN neurons recorded in the different animals showed two distinct distributions of neurons, with one rostral group and one caudal group (Fig. 1*C* and *D*).

Data acquisition

Unit activity was sampled at 10 kHz. The ECoG signal was sampled at 5 kHz. The ECG and respiration signals were each sampled at 400 Hz. All biopotentials were digitized on-line with a PC running Spike2 acquisition and analysis software (version 4; Cambridge Electronic Design Ltd, Cambridge, UK).

Peristimulus time histograms and cusums

The short-latency (<200 ms) responses of units to cortical stimulation were analysed by peristimulus time histograms (PSTHs). These were constructed for each STN unit from 210 consecutive stimulation trials (Magill *et al.* 2004*a*). The timings of changes in single unit activity were

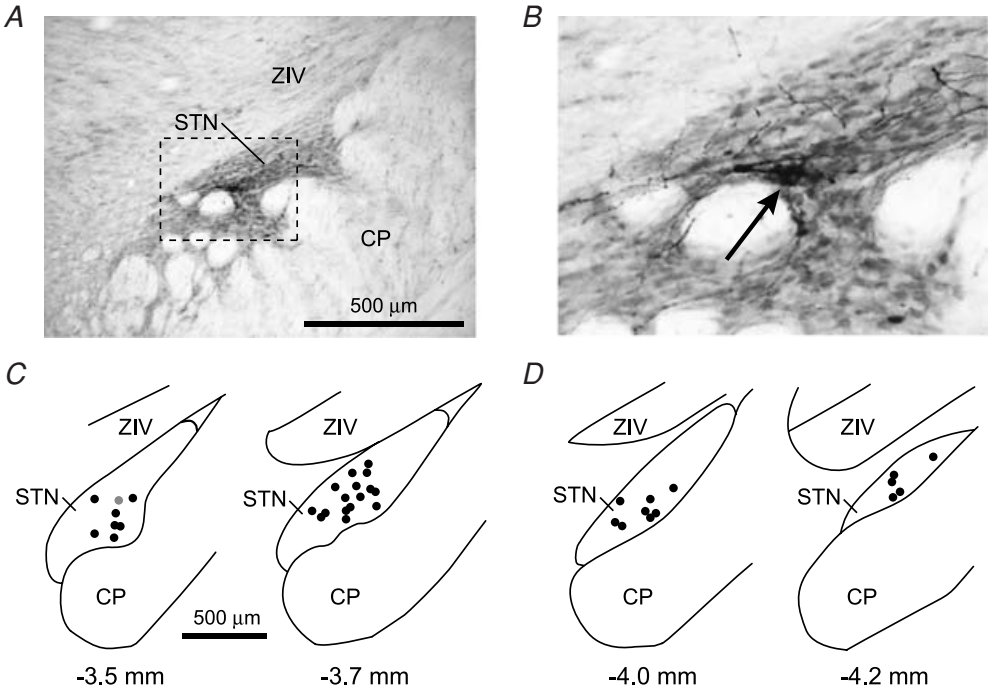

Figure 1. Locations of recorded subthalamic nucleus neurons
A, digital micrograph of a typical Neurobiotin deposit that marked a recording location in the rostral half of the subthalamic nucleus (STN). Tissue section cut in the coronal plane (dorsal towards the top, lateral to the right). The STN is characterized by a higher density of neurons compared to the overlying ventral division of the zona incerta (ZIV). CP, cerebral peduncle. *B*, area in *A* within the dashed box shown at greater resolution. The core of the Neurobiotin deposit is identified as a dense accumulation of black reaction product (arrow), which is accompanied by Golgi-like labelling of neighbouring neurons. *C*, locations of all 24 neurons recorded in the rostral half of the STN, plotted in the coronal plane. The number below each section corresponds to the distance posterior of bregma. Location shown in *A* is highlighted as a grey circle. *D*, locations of all 13 neurons recorded in the caudal half of STN. Scale bar in *C* also applies to *D*.

determined by change-point analysis, using commercial software (Change-Point Analyser 2.0 shareware program, http://www.variation.com/cpa/tech/changepoint.html), and techniques previously described (Cassidy *et al.* 2002; Williams *et al.* 2003). Change-point analysis iteratively uses a combination of time-varying cumulative sum charts ('cusums'; see Ellaway, 1978) and random re-ordering of the original data (bootstrapping) to set confidence limits for the cusum of the original data set (Change-Point Analyser 2.0 shareware program). PSTHs of unit activity from 200 ms before, to 400 ms after cortical stimuli were first plotted with 1 ms bins. Cusums were then determined by plotting the sequentially summed deviations from the average discharge count per millisecond determined from the whole record segment (total of 600 ms), as this affords a more conservative estimate of significant changes than the use of any *a priori* defined control period. One thousand bootstraps were performed in each test and only changes with probabilities of $\leq$0.05 were considered significant. Upward gradients in cusums denote increases in discharge rate, whereas downward gradients denote decreases in discharge rate. The mean discharge count per millisecond over each identified interval of significant change was calculated and expressed as a percentage of the mean prestimulus (background) discharge count per millisecond, which was estimated from 200 to 0 ms before cortical stimulation. A reduction in firing was considered complete if mean activity over the period of reduced discharge identified by change point analysis was $<$5% of background activity.

Time-domain representations of coupling between STN unit activity and ECoG were determined by histograms using only the first action potential fired in the series of delayed oscillatory STN unit discharges that followed the prolonged period of reduced activity, or a long pause in firing, while at the same time reducing the ECoG signal to a digital representation of consecutive positive peaks. The latter was achieved by automatically selecting all ECoG peaks of an amplitude greater than 0.1 mV, with a minimum interval of 3 ms, using the peak-detection function of Spike2 after the ECoG had been first smoothed using a moving-average filter that averaged five consecutive data points before shifting one data point and repeating the procedure. The ECoG data were searched for all peaks that were followed by a fall in voltage of at least 0.1 mV. The criterion for detection was thus a 'peak-to-trough' amplitude of 0.1 mV. Only positive peaks were considered for the analysis. Spike-triggered averages (STAs) of ECoGs were also calculated, after first discriminating STN unit discharges to give a digital signal.

Coherence and phase analyses

The long-latency, 'delayed' ($>$200 ms) effects of cortical stimulation were characterized by frequency analysis of point process data (STN unit discharge) and time series data (cortical activity). For example applications of this technique to similar signals in neurophysiological studies see Brown *et al.* (1999) and Halliday *et al.* (1999). Point process unit activity in STN was downsampled to 5 kHz to match the ECoG. Two periods of unit activity and simultaneously recorded ECoG of 410 ms duration were exported for frequency analysis: 205–615 ms and 1024–1434 ms after cortical stimulation. These 410 ms windows were the minimum that afforded reasonable frequency resolution (2.4 Hz) in the coherence and phase analyses. The first window, with an onset of 205 ms after stimulation, approximated, on the whole, to the timing and duration of robust oscillatory responses in the cortex and subthalamic nucleus. The latter window, with onset 1024 ms after stimulation, was chosen to test whether oscillatory activity and corresponding coherence was short-lived and recovered prior to the next electrical stimulus in the train. Both periods so chosen involved response elements with local stationarity in the STN and ECoG signals. Unit activity and ECoG were examined after 210 cortical stimuli, so this gave 86.1 s of data for each of these periods. Time-series data, describing STN unit activity and ECoG activity during the 205–615 ms and 1024–1434 ms epochs, were separately concatenated and analysed in the frequency domain using blocks of 2048 data points (410 ms), which exactly corresponded to the exported sections. Data were passed through a Hanning window filter so that discontinuities between successive concatenated blocks were suppressed. Contiguous data sections of 10–28 s (mean duration 16 s) were also drawn from recordings of spontaneous activity made immediately prior to the start of the train of 210 cortical stimuli in the 15 STN units that exhibited responses to corticosubthalamic input and had $>$10 s of spontaneous activity recorded before stimulation. As the duration of recording of spontaneous activity varied between units and never reached 86.1 s, spontaneous activity was separately compared to stimulation periods of matching duration for each unit.

The ECoG, denoted by $_{\mathrm{A}}$, was assumed to be a realization of a stationary, zero-mean time series. Unit activity in STN was assumed to be a realization of a stationary, stochastic point process and was denoted by $_{\mathrm{B}}$ (Perkel *et al.* 1967). Both processes were further assumed to satisfy a mixing condition, whereby sample values widely separated in time were independent (Brillinger, 1981). The principal statistical tool used for the data analyses was the discrete Fourier transform and parameters derived from it, all of which were estimated by dividing the records into a number of disjointed sections of equal duration (2048 data points, affording a frequency resolution of 2.4 Hz). Spectra were estimated by averaging across these discrete sections (Halliday *et al.* 1995). In the frequency domain, estimates of the power spectra of the ECoG, $f_{\mathrm{AA}}(\lambda)$, and unit

activity, $f_{BB}(\lambda)$, were constructed, along with estimates of coherence, $|R_{AB}(\lambda)|^2$, between the ECoG and unit activity. The coherence was calculated according to:

$$|R_{AB}(\lambda)|^2 = \frac{|f_{AB}(\lambda)|^2}{f_{AA}(\lambda) f_{BB}(\lambda)}$$

where λ denotes the frequency, and $f_{AB}(\lambda)$ is the cross spectrum between $_A$ and $_B$. Confidence levels (95% CL) for coherence spectra were determined according to methods described in Halliday *et al.* (1995). A peak of significant coherence in the spectrum was defined as >2 contiguous frequency bins (i.e. >4.8 Hz in duration) above the 95% CL, provided that the onset frequency of the peak was >4.8 Hz. The latter criterion was included so as to distinguish coherence due to slow shifts in the DC potential from discrete peaks of coherence at higher frequencies.

Phase, ϕ_{AB}, defined as the argument of the cross spectrum, is:

$$\phi_{AB}(\lambda) = \arg[f_{AB}(\lambda)]$$

The phase estimated from a single point (e.g. frequency) is ambiguous. Measuring phase relationships that are linear over a band of frequencies reduces this ambiguity (Gotman, 1983). Under these circumstances, the temporal delay between the signals can be calculated from delay (ms) $= g \times (1/2\pi)$, where g is the gradient of the line in plots of phase (radians) against frequency (Hz). A negative gradient indicates that the input/reference signal leads. The constant time lag between the STN unit discharge and ECoG could be calculated from the slope of the phase estimate after a line had been fitted by linear regression in seven spectra from seven units, from which the corresponding coherence estimates had a total of eight significant peaks (one spectrum had two peaks; coherence determined as significant where it exceeded the 95% CL as determined above). These peaks had >4 contiguous frequency bins and linear regression of the phase estimates established a $r^2 > 0.65$ and a $P < 0.05$.

Statistics

Linear correlation was tested by Pearson's correlation coefficient (unless otherwise stated). All *t* tests, Fisher Exact tests, χ^2 tests, and tests of the significance of correlation coefficients were two tailed. Significance was considered as $P < 0.05$.

Results

The spontaneous activities of STN neurons were similar to those previously described (Magill *et al.* 2000, 2001, 2004*a*), i.e. mean firing rates of ~10 Hz, but with a variety of firing patterns. The spontaneous activity of STN neurons and their responses to cortical stimulation were recorded during the whole gamut of brain states commonly observed in the ECoG of urethane-anaesthetized rats, including 'slow-wave activity', spontaneous (global) 'activation', and mixtures thereof (see Magill *et al.* 2000, 2004*b*). Accordingly, STN neurons tended to fire bursts of spikes in a periodic manner (~1 Hz) during slow-wave activity, whereas they tended to discharge with tonic, irregular patterns during the activated brain state (Magill *et al.* 2000).

As reported previously, the responses of STN neurons to cortical stimulation are often 'multiphasic' (Kitai & Deniau, 1981; Ryan & Clark, 1992; Fujimoto & Kita, 1993; Maurice *et al.* 1998; Nambu *et al.* 2000; Kolomiets *et al.* 2001; Magill *et al.* 2004*a*). Such multiphasic responses can include, in order of temporal evolution, a short-latency excitation, a brief reduction in firing, a secondary excitation (a combination hereafter referred to as a 'short-latency triphasic response'), a prolonged reduction in firing and, finally, a delayed recovery of activity. Because the short-latency triphasic responses of STN units to electrical stimulation of the ipsilateral frontal cortex, as described here, have been previously reported in the same animals (Magill *et al.* 2004*a*), and given that these early response phases have also been described in detail by others (see above), they will only be briefly summarized below.

Responses of units recorded in rostral STN to stimulation of frontal cortex

Peristimulus time histograms of the responses of 24 units in rostral STN (Figs 1*C* and 2*A*) to electrical stimulation of the ipsilateral frontal cortex demonstrated a short-latency triphasic pattern, beginning with an excitation of a mean latency of 4.3 ms (S.D. 2.0 ms) that was followed by a brief period of suppressed firing and then another excitation. This short-latency triphasic response was in turn followed at 33 ms (S.D. 19 ms) by a prolonged silencing of unit discharge. Thereafter, upon recovery from this prolonged quiescence at around 200 ms, unit discharges had a tendency to occur at periodic intervals for up to 650 ms after stimulation, evident over the 200–650 ms period as a series of peaks and troughs in PSTHs (Fig. 2*A*). These were mirrored by undulations in the frontal cortical ECoG over the same period but tended to dampen thereafter (Fig. 2), such that ECoG 'peaks' (see Methods) were only very rarely detected between 650 and 1450 ms after stimulation. At the range of stimulation current amplitudes used here, which ensured maximal responses (see Methods), these delayed unit responses and ECoG undulations did not systematically differ with gross fluctuations in brain state (as assessed from the ECoG), in agreement with our previous finding that short-latency triphasic responses evoked during slow-wave activity did not differ substantially from those evoked during global activation

(see Magill *et al.* 2004*a*). However, although these delayed responses were observed in recordings made during either slow-wave activity or global activation, the two extremes of brain state observed in this preparation (Magill *et al.* 2004*b*), we were unable to make direct comparisons of the evoked responses of any one rostral STN neuron, together with those of a single cortical locus, during both brain states.

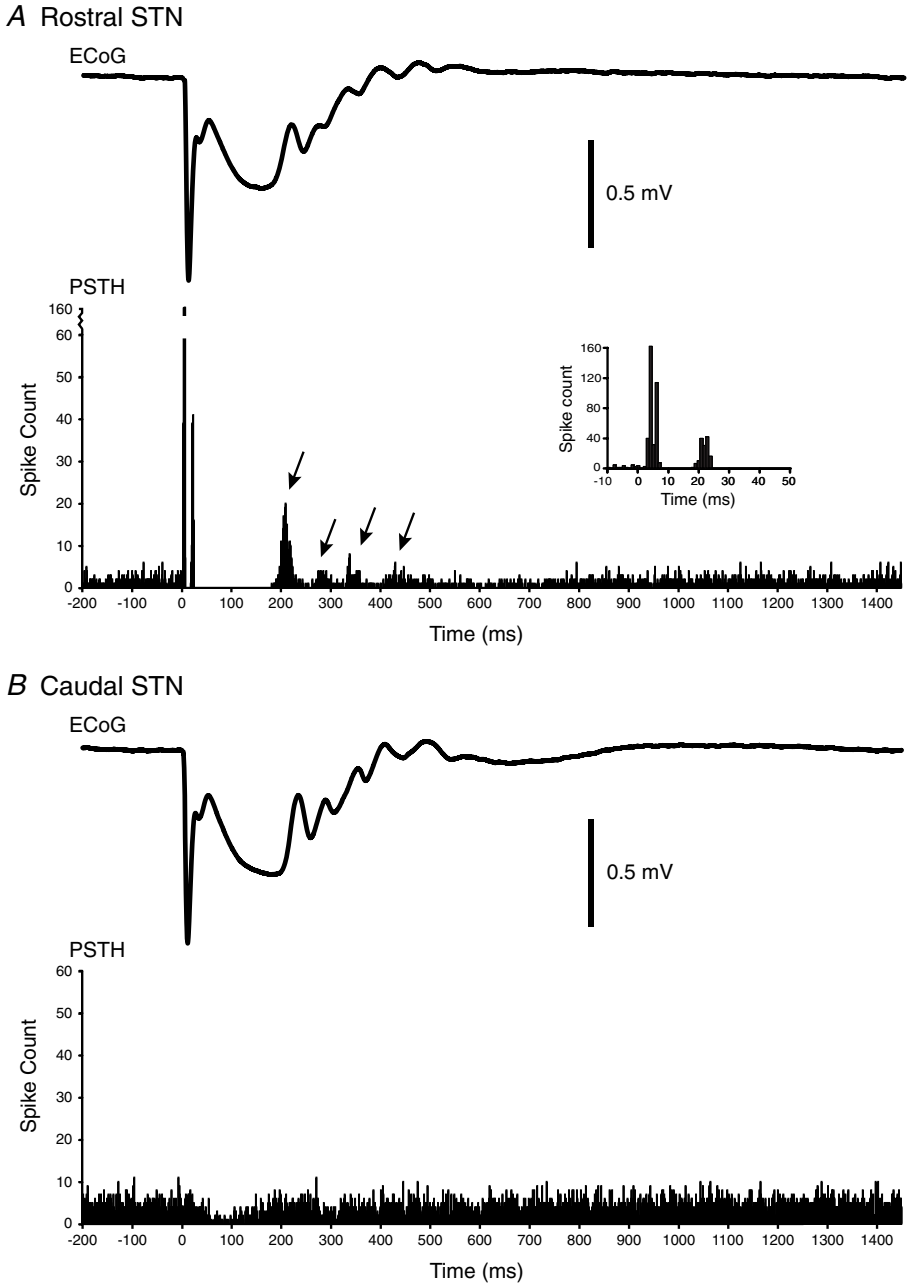

Figure 2. Typical examples of the averaged responses of subthalamic nucleus neurons to frontal cortical stimulation

A, typical rostral subthalamic nucleus (STN) unit. Lower trace, the peristimulus time histogram (PSTH) aligned to cortical stimuli at $t = 0$ ms. The stereotypical short-latency triphasic response (excitation, inhibition and excitation; see inset) is followed by a prolonged pause in firing. The pause terminates after about 200 ms and is followed by unitary discharge that tends to cluster at certain times (arrows). The repetitive peaks and troughs in unit activity are mirrored by undulations in the electrocorticogram (ECoG) averaged with respect to cortical stimuli at $t = 0$ ms, as shown in the upper trace. Note that these delayed oscillatory responses in STN and the ECoG tended to dampen at around 600 ms after stimulation. Polarity of ECoG is displayed as positive up. *B*, typical caudal STN unit in same animal (rat 227) in response to cortical stimulation at the same site. Lower trace, the PSTH aligned to cortical stimuli at $t = 0$ ms. There is no short-latency triphasic response, but there is a prolonged period of reduced firing that terminates after about 200 ms. There is no clear clustering of subsequent unit activity. Despite this, undulations are visible in the averaged ECoG.

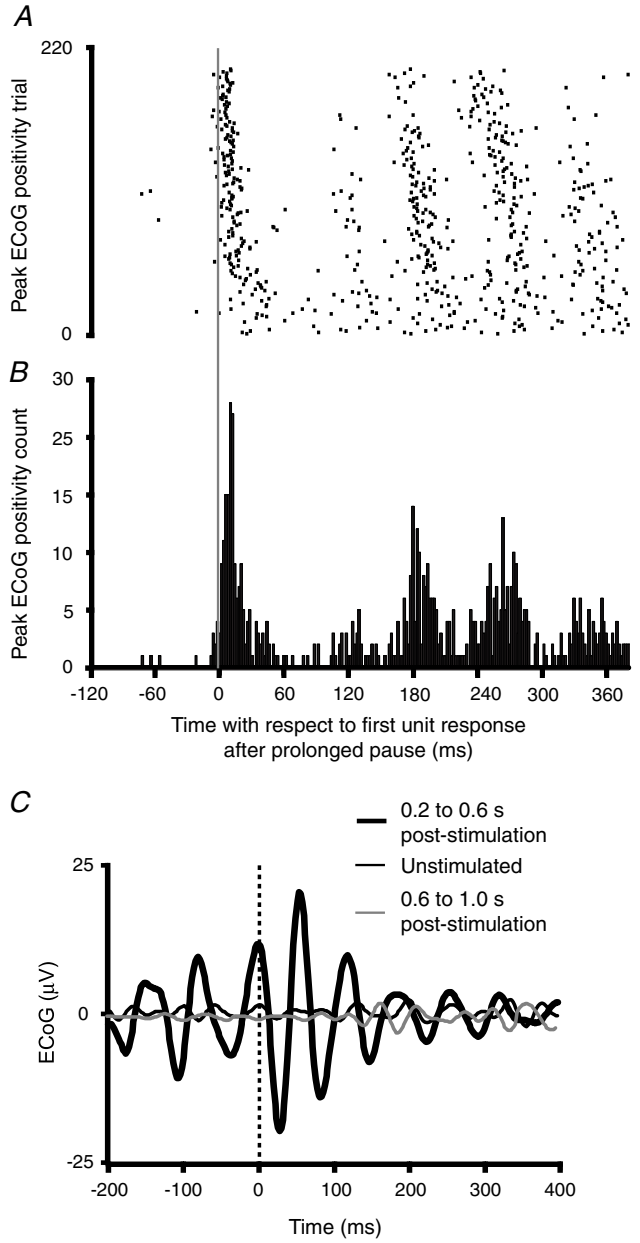

Figure 3. Time-domain analyses of the relationship between delayed responses of ECoG and a STN unit
A, raster, and *B*, histogram, of the timings of consecutive positive peaks in the ECoG with respect to the timing of the first action potential fired in the series of delayed oscillatory STN unit discharges following the prolonged pause in firing. Same rostral STN unit as shown in Fig. 2*A* after electrical stimulation of the frontal cortex. The vertical grey line at 0 ms represents the first action potential of the STN unit. Note that most oscillatory cortical events follow STN neuronal discharge after stimulation of the frontal cortex. *C*, spike-triggered averages (STAs) of ECoG for same STN unit performed over different time intervals with respect to frontal cortical stimuli. All spikes that occurred within the respective time periods were used for averaging the ECoG. Spikes of STN neuron aligned at $t = 0$ ms (dashed line). The STA from the period 0.2–0.6 s following cortical stimuli is clearly oscillatory, with the peak cortical activity lagging behind STN unit activity on average (displaced to the right of $t = 0$ ms). Polarity of ECoG is displayed as positive up.

The timings of these delayed peaks and troughs in PSTHs of unit discharge relative to undulations in the ECoG are difficult to ascertain. Figure 3*A* and *B* shows that at least the first action potential discharged by STN neurons after the delayed and prolonged pause in firing can precede the onset of the repetitive peaks in the ECoG (peaks of amplitude greater than 0.1 mV, see Methods). Here, a histogram of the timings of consecutive positive peaks in the ECoG has been plotted with respect to the timing of the first action potential fired in the series of delayed oscillatory STN unit discharges following the prolonged pause in activity. However, although there is a clear lead of the STN discharge over the repetitive peaks in the ECoG, this analysis is not informative of temporal relationships throughout the oscillatory period, and is itself subject to the arbitrary selection of the phase of the cortical wave to be represented (peak or trough). An alternative approach is to estimate the STA of the ECoG during the delayed oscillatory period. The STAs for the STN unit illustrated in Fig. 3*A* and *B* show that, during the period 200–600 ms after stimulation (but not later periods), STN and ECoG activities are clearly oscillatory, with the peak positivity of the ECoG lagging unitary discharge (Fig. 3*C*). However, STAs tend to be dominated by higher amplitude, low-frequency components in the ECoG, so that oscillatory relationships in the frequency band of interest are not always so clear (see Magill *et al.* 2004*b*).

The above limitations of such time-domain analysis may be circumvented by frequency analysis. Spectra of the coherence between STN unit discharges and ECoG over the period of 205–615 ms after stimulation demonstrated one or more significant peaks of activity at 5–30 Hz (Fig. 4*C* and *G*). Note that peaks were not seen at serial harmonics of the frequency of cortical stimulation (Fig. 4*C* and *G*). It is also unlikely that peaks in coherence at higher frequencies were harmonics of peaks at other low frequencies. Most significant peaks were single, and in the seven spectra where two discrete peaks of coherence were present, there was no significant correlation between the frequencies of maximum coherence of the first and second peaks (Pearson's correlation, $r = 0.67$, $P = 0.10$). Note also that there was no significant linear correlation between the mean background discharge frequency of each neuron recorded in rostral STN and the peak coherence between unit activity and ECoG over the period 200–650 ms after cortical stimulation (Pearson's correlation, $r = -0.12$, $P = 0.59$). This lack of correlation is also evident in Fig. 4 (compare *B* with *C*, and *F* with *G*). There were no significant peaks in the spectra of the coherence between STN unit discharges and ECoG over the period of 1024–1434 ms after stimulation (Fig. 4*C* and *G*), during which peaks/troughs in unit activity and undulations in ECoGs were of negligible amplitudes (Fig. 2). Thus, the increase in coherence following cortical stimulation was temporary, such that significant coherence had almost

disappeared by 1 s after stimulation (Fig. 5*A*, Fisher Exact test, $P < 0.0001$, comparing data over 5–30 Hz). Furthermore, the elevated coherence between STN unit activity and ECoG present 205–615 ms after stimulation was not apparent prior to cortical stimulation. This was confirmed by comparing the coherence between STN unit activity (15 neurons) and ECoG prior to stimulation with the coherence present in a comparable number of data sections taken 205–615 ms after stimulation (Fig. 5*B*). Coherence over 5–30 Hz was significantly higher at 205–615 ms after stimulation compared to before stimulation (Fisher Exact test, $P < 0.0001$).

In spectra from seven STN units, it was possible to estimate the phase of coherence between STN unit activity and ECoG in the 205–615 ms period after stimulation by linear regression (Fig. 4*D* and *H*, and Table 1; eight phase estimates in total because one unit had two peaks of coherence). These phase plots demonstrated that the STN unit discharges preceded ECoG waves by a mean interval of 28.6 ms (s.d. 11.8 ms) over a total frequency range of approximately 7–32 Hz in these units (Table 1). The phase estimates included the data set used for the time-domain analysis shown in Fig. 3, and confirm that the temporal lead of the STN unit over ECoG following the prolonged pause in firing was representative of the whole cycle of the oscillatory waveform and of the whole period 205–615 ms after stimulation in these units. Phase estimates at frequencies of significant coherence in the remaining units were mixed. In the latter instances, phase estimates across frequencies were not modelled by a linear relationship.

Responses of units recorded in caudal STN to stimulation of frontal cortex

To investigate the topography of frequency relationships between cortex and STN, we also recorded the responses of neurons in the caudal half of STN ($n = 13$; Fig. 1*D*). The responses of neurons located in rostral and caudal STN to stimulation of the frontal cortex were different (see Magill *et al.* 2004*a*). No short-latency triphasic responses were seen in the PSTHs of caudal STN units (Fig. 2*B*). A delayed and prolonged reduction in firing was present in all but one caudal STN neuron, but the reduction was less than that displayed by rostral STN units (mean discharge frequency of caudal STN units fell to 73% (s.d. 18%) of baseline, as compared to complete quiescence for rostral units). The mean onset latency of this reduced firing, as determined from cusums, was 37 ms (s.d. 11 ms), which was not significantly different from the mean onset latency of the delayed pause in activity exhibited by rostral STN units (unpaired *t* test). The mean durations of the sustained periods of reduced firing, as determined from cusums, were also similar (unpaired *t* test; 236 ms (s.d. 86 ms) for caudal units and 232 ms (s.d. 54 ms) for rostral units). The appearance of the mean ECoG waveform after frontal cortical stimulation did not differ in experiments in which units were recorded in rostral and caudal STN (Fig. 2*A* and *B*). In particular, the same undulations were evident in the frontal ECoG at 200–650 ms after cortical stimuli (Fig. 2*B*). Despite these apparent similarities, the tendency for the discharges of caudal STN units to occur at periodic intervals immediately following recovery from reduced discharge was less marked as compared to rostral STN units (cf. Figure 2*A* and *B*). Accordingly, spectra of the coherence between unit discharges in caudal STN and frontal ECoG over the period of 205–615 ms after stimulation demonstrated fewer significant peaks, particularly at those frequencies above 15 Hz (Fig. 5*C*). Comparison of the coherence spectra of rostral STN units and caudal STN units revealed that there was no difference in the incidence of significant coherence below 15 Hz, but there was a significant difference over the 15–30 Hz range (χ^2 test, $P < 0.00001$), such that rostral STN units exhibited a proportionally greater incidence of coherence above 15 Hz.

Responses of units recorded in rostral STN to stimulation of temporal cortex

To determine whether the coherence profiles over the period of 205–615 ms after stimulation were relatively specific to stimulation of the frontal cortex, we also recorded the responses of some of the same rostral STN units ($n = 12$ of 24) to stimulation of the ipsilateral temporal cortex. Stimulation of temporal cortex did not produce short-latency triphasic responses in PSTHs of rostral STN units, and only one neuron demonstrated the delayed and prolonged reduction in firing. The grouping of unit discharges at periodic intervals over the 200–650 ms period after stimulation were diminished as compared to responses to frontal cortical stimulation, and the delayed undulations were absent from the frontal ECoG. Accordingly, there was a significant reduction (χ^2 test, $P < 0.00001$) in coherence between STN unit activity and frontal ECoG over 5–30 Hz after temporal cortical stimulation as compared to frontal stimulation (Fig. 5*D*). Furthermore, phase relationships of coherence over 5–30 Hz were mixed after temporal cortex stimulation, so that phase spectra could not be fitted by a linear model. Thus, electrical stimulation of the temporal cortex was relatively ineffective in eliciting coherence between unit activity in the rostral STN and frontal ECoG.

Responses of units recorded in caudal STN to stimulation of temporal cortex

To further define the functional specificity of evoked coherence, we recorded the responses of some of the same units in caudal STN ($n = 9$ of 13) to stimulation

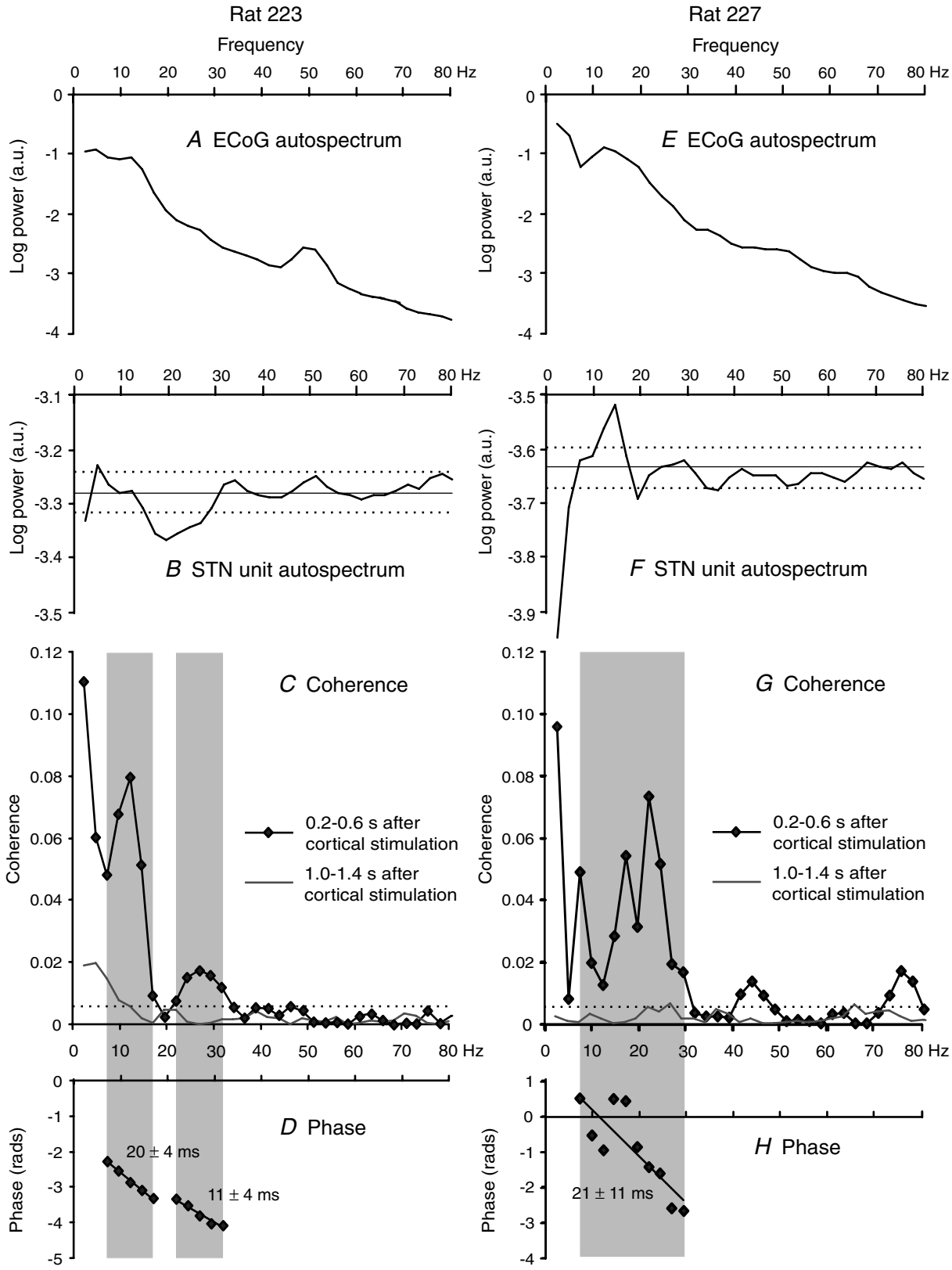

Figure 4. Frequency analysis of the responses of rostral STN units and frontal ECoGs to frontal cortical stimulation in two representative rats

A–D, ECoG autospectrum (*A*), STN unit autospectrum (*B*), coherence (*C*) and unconstrained phase (*D*) relationships between a STN unit (point process, 1518 spikes from 0.2 to 0.6 s after stimulation) and ipsilateral ECoG (analog

of ipsilateral temporal cortex. Stimulation of temporal cortex did not elicit short-latency triphasic responses in the PSTHs of caudal STN units. However, all but one neuron demonstrated a delayed reduction in firing in response to stimulation. The mean onset latency of this reduction, as determined from cusums, was 44 ms (S.D. 24 ms), which was not different from the onset latency of the delayed reduction in firing in caudal STN units following frontal cortex stimulation (unpaired *t* test). The mean duration of the periods of reduced firing was also similar (279 ms (S.D. 69 ms); unpaired *t* test). The mean discharge frequency of caudal STN units fell to 66% (S.D. 12%) of baseline levels during these delayed reductions in firing. The tendency for unit discharges in the caudal STN to occur at periodic intervals over the 200–650 ms period after stimulation of the temporal cortex was not as clear as in the rostral STN following stimulation of the frontal cortex. Undulations were virtually absent in the frontal ECoG following stimulation of temporal cortex. Coherence between unit activity in caudal STN and ECoG in the period of 205–615 ms after stimulation did not differ to that seen following frontal cortex stimulation over the 5–30 Hz band (χ^2 test, $P > 0.05$), as illustrated in Fig. 5*E*. Thus, electrical stimulation of the temporal and frontal cortices was equally (in)effective in eliciting coherence between frontal ECoG and unit activity in the caudal STN. However, coherence at 5–30 Hz was still significantly less than that recorded in rostral STN following frontal cortex stimulation (χ^2 test, $P < 0.0001$).

Correlation of the coherence between STN units and frontal ECoG at 5–15 Hz with the delayed reductions in firing rate

Coherence between unit activity and ECoG at frequencies above 15 Hz was thus largely restricted to those STN neurons exhibiting a typical, short-latency triphasic response to frontal cortical stimulation, including a brief short-latency excitation response indicative of direct corticosubthalamic input arising from the region of stimulated cortex. Coherence between STN units and ECoG below 15 Hz was more widely distributed in STN, as was the case for the delayed and sustained reductions in firing. Coherence at 5–15 Hz was elicited following stimulation of either the frontal or temporal cortices, although the strongest coherence tended to occur in the rostral STN after frontal cortical stimulation. Accordingly, we correlated the degree of significant coherence in the 5–15 Hz band with the magnitude of the delayed reductions in firing elicited by frontal and temporal cortical stimulation in all 58 recordings (including those in which the same unit was studied after stimulation of the frontal and temporal cortex). Coherence was greater when the reduction in unit activity within STN was greater (Spearman's rho 0.481, $P < 0.001$). This correlation was not significant when only units in rostral STN were considered (because most units were recorded following stimulation of the frontal cortex, when the reduction in firing was complete and neurons were silent). However, when only units in caudal STN were considered, coherence was again greater when the reduction in unit activity within STN was greater in magnitude (Spearman's rho 0.478, $P < 0.01$).

Discussion

This study is the first to examine in detail the delayed (>200 ms) responses of STN neurons to synchronized cortical output. Our results show that following cortical stimulation and a prolonged reduction in firing, STN neurons often display a delayed, and temporary, oscillatory discharge that is coherent with the population activity recorded in the frontal ECoG. Coherent activity in STN and cortex occupied a broad frequency band of 5–30 Hz, and varied according to the locations of neurons in STN and the area of cortex stimulated, and thus, topography and function. Coherence with ECoG at 5–15 Hz was observed throughout STN, following both frontal and temporal cortex stimulation. However, coherence with ECoG at 15–30 Hz was effectively limited to the delayed responses of rostral STN units to stimulation of frontal cortex. Thus, delayed coherence was organized in a

data, 82 s, 210 stimuli) in rat 223. Note that *A* has a 50 Hz mains artefact. *C* also shows coherence between same unit (1087 spikes) and ECoG during the 1.0–1.4 s period after stimulation. *E–H*, ECoG autospectrum (*E*), STN unit autospectrum (*F*), coherence (*G*) and unconstrained phase (*H*) between a STN unit (599 spikes from 0.2 to 0.6 s after stimulation) and ipsilateral ECoG (82 s, 210 stimuli) in a different rat (rat 227, as illustrated in Figs 2*A* and 3). *G* also shows coherence between the same unit (599 spikes) and ECoG 1.0–1.4 s after stimulation. Resolution of all spectra is 2.4 Hz. Dashed lines represent the 95% confidence levels (CLs) (except for ECoG power spectra where 95% CLs were <0.1). Grey shading in coherence plots defines peaks determined using our criteria (see Methods). Two peaks in coherence are evident from about 7–17 and 22–31 Hz in data drawn from 0.2 to 0.6 s after cortical stimulation in *C* (two peaks of significant coherence with at least 4 contiguous frequency bins in each peak were seen in only 3 spectra) and one broad peak from about 7–30 Hz in *G*. The corresponding phase estimates show consistent cortical lags (negative gradient) equivalent to 20 ± 4 ms (±95% CL) and 11 ± 4 ms in *D*, and 21 ± 11 ms in *H*. Note that peaks in coherence (*C* and *G*) did not correspond to peaks in unit discharge frequency (*B* and *F*), and that there were no significant peaks in coherence at 1.0–1.4 s after cortical stimulation in *C* or *G*. a.u., Arbitrary units

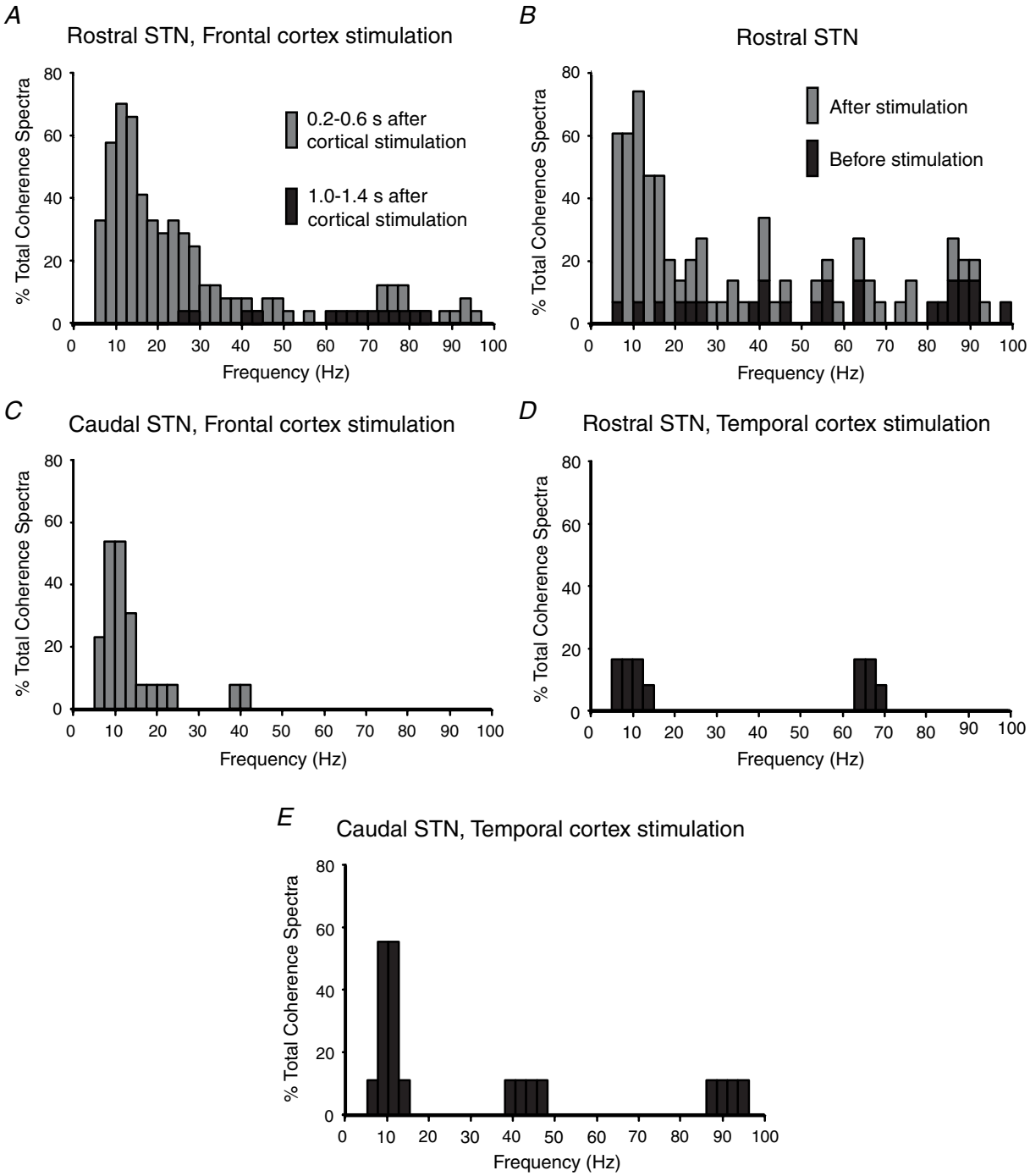

Figure 5. Summary of the coherence between frontal ECoG and activity of units in rostral and caudal STN as a function of time before and after, and site of, cortical stimulation

The percentages of total coherence spectra classified as containing significant coherence within a given frequency bin (2.4 Hz) are shown. *A,* coherence between activity of units in rostral STN and frontal ECoG as a function of time after frontal cortical stimulation. Data are derived from 24 STN units in rostral STN that showed short-latency triphasic (i.e. corticosubthalamic) responses to stimulation. Coherence is much more evident at 0.2–0.6 s than at 1.0–1.4 s after stimulation. *B,* comparison of coherence between activity of single units in rostral STN and frontal ECoG before stimulation and 0.2–0.6 s after stimulation of frontal cortex. Data are derived from 15 units in rostral STN that exhibited short-latency responses to stimulation and for which >10 s of data before stimulation were available. Data lengths were matched for records before and after stimulation in each case. Coherence is much more common following cortical stimulation. *C,* coherence between activity of single units in caudal STN and ECoG during the period of 0.2–0.6 s after stimulation of frontal cortex. Data were derived from 13 units in caudal

Table 1. Phase relationships between activity of rostral STN units and frontal ECoG

Record no.	Frequency range (Hz)		*n*	r^2	*P* value	STN lead (Y/N)	Latency (ms) (±95%CL)
228 m	12.2	29.3	8	0.985	<0.00001	Y	41 ± 5
228r	7.3	17.1	5	0.814	0.0361	Y	39 ± 26
223k1	9.8	22	6	0.927	0.0021	Y	39 ± 15
228b	17.1	26.9	5	0.852	0.0253	Y	20 ± 15
227aa	17.1	29.3	6	0.890	0.0047	Y	38 ± 18
223b2	7.3	17.1	5	0.994	0.0028	Y	20 ± 4
223b2	22	31.7	5	0.915	0.0028	Y	11 ± 4
227z	7.3	29.3	10	0.679	0.0034	Y	21 ± 11
Mean	12.5	25.3	6.3				28.6
S.D.	5.6	5.8	1.8				11.8

STN, subthalamic nucleus; *n*, number of data points used in linear regression analysis. Note that unit 223b2 showed two peaks of coherence with electrocorticogram (ECoG; shown in Fig. 4*C*) so that two phase estimates were possible (see Fig. 4*D*).

topographic and functionally relevant manner (cf. rostral *versus* caudal STN, and cf. inputs from frontal *versus* temporal cortex). The phase relationship between cortical and STN activity was most often mixed, but there were several clear examples of STN *leading* cortex. Indeed, oscillatory responses at 5–30 Hz in rostral STN led those in cortex with a mean latency of 29 ms, but only after frontal cortical stimulation. This temporal relationship could have arisen due to common input(s) influencing both neurons in rostral STN and frontal cortex, but with shorter delays to the former. However, given the looping architecture of the basal ganglia-thalamocortical pathways, and the mean time difference, it seems more plausible that this temporal relationship was mediated via polysynaptic pathways from the basal ganglia to the cortex.

Synaptic inputs and intrinsic mechanisms underlying the short-latency and delayed responses of STN neurons to stimulation

The STN receives monosynaptic inputs from select areas of the ipsilateral cerebral cortex, including prefrontal, premotor, primary motor and somatosensory areas (see review by Smith *et al.* 1998). Neurons in the rostral half of STN typically responded to stimulation of the ipsilateral frontal (sensorimotor) cortex with a short-latency triphasic pattern of activity, as previously described in the same paradigm (Magill *et al.* 2004*a*). The first phase of the short-latency triphasic response was a brief, but powerful, excitation, which appears to be driven by the direct, excitatory corticosubthalamic projection (Kitai & Deniau, 1981; Ryan & Clark, 1992; Fujimoto & Kita, 1993; Maurice *et al.* 1998; Nambu *et al.* 2000; Kolomiets *et al.* 2001). The second and third phases of the typical unit response develop from polysynaptic interactions (see Fujimoto & Kita, 1993; Maurice *et al.* 1998; Bevan *et al.* 2002*b*). The accompanying short-latency responses of the ECoG to frontal cortical stimulation were almost certainly due to direct orthodromic and antidromic excitation of intracortical and corticopetal neuronal elements (Oldfield & Castro-Alamancos, 2003).

Units recorded in the rostral half of STN did not display a short-latency triphasic response to stimulation of ipsilateral temporal cortex, which is in keeping with studies demonstrating that the (auditory) temporal cortex does not project *directly* to STN (Canteras *et al.* 1990; Kolomiets *et al.* 2001). The topographical organization of unit responses was not only evident with respect to cortical areas, but also within the STN itself. Neurons located in the caudal half of STN did not respond at short latency to stimulation of either frontal or temporal cortex. These findings are in agreement with previous anatomical (Canteras *et al.* 1990; Kolomiets *et al.* 2001) and physiological (Kolomiets *et al.* 2001; Magill *et al.* 2004*a*) studies, which have shown that the frontal cortical areas stimulated

STN. Coherence with ECoG, and especially that above 15 Hz, is much less common in caudal STN as compared to rostral STN (see *A*). *D,* coherence between activity of single units in rostral STN and frontal ECoG during the period of 0.2–0.6 s after stimulation of temporal cortex. Data were derived from 12 units in rostral STN. Coherence with ECoG at 5–30 Hz is not common in rostral STN following temporal cortex stimulation. *E*, coherence between activity of single units in caudal STN and frontal ECoG during the period of 0.2–0.6 s after stimulation of temporal cortex. Data were derived from 9 units in caudal STN. Coherence with ECoG is equally as common in caudal STN following stimulation of either temporal or frontal cortices (cf. *E* and *C*), but is only prominent in the 5–15 Hz band.

in the present study project to the rostral two-thirds of STN only. Importantly, response differences were unlikely to be due to insufficient current flow at the site of stimulation because responses should have been maximal, with respect to pattern, at the stimulus intensities used (Magill *et al.* 2004*a*).

A prolonged reduction in activity, albeit of varying intensity, frequently preceded the delayed oscillatory responses of neurons in both rostral and caudal aspects of STN, which were, in turn, associated with increased coherence with cortex in the 5–30 Hz range. With one exception, neurons in rostral STN did not demonstrate a sustained reduction in activity after stimulation of temporal cortex, and their delayed oscillatory activity in response to the same stimulus was only weak (and weakly coherent with cortex at 5–15 Hz). The most robust unit activity oscillations and strongest coherence with cortex were characteristic of the rostral STN neurons that were consistently and completely silenced following frontal cortical stimulation. However, a prolonged reduction in the activity of STN units alone was not a requisite for the generation of subsequent coherent oscillations at 15–30 Hz. Although many STN units displayed coherent oscillations after stimulation, coherence at 15–30 Hz was almost exclusive to rostral STN in response to inputs from frontal cortex.

The cellular and synaptic mechanisms underlying the prolonged reduction or pause in firing are unknown, as are the factors responsible for generating the delayed oscillatory activity of STN neurons. A 'disfacilitation' of cortical inputs has been hypothesized to be the cause of the prolonged reduction in firing (Fujimoto & Kita, 1993; Kita, 1994; Nambu *et al.* 2002). Yet, this interpretation does not fit well with extracellular recording data showing that many STN neurons are not silenced by acute ablation of much of the ipsilateral frontal and parietal cortices (Magill *et al.* 2001). The cumulative activation of Ca^{2+}-dependent K^+ channels during the third (excitation) phase of the short-latency triphasic response, eventually leading to a prolonged 'afterhyperpolarization', might also have contributed in some neurons (Beurrier *et al.* 1999; Bevan & Wilson, 1999; Hallworth *et al.* 2003). More recent *in vitro* data suggest that the delayed pause in firing could also be a reflection of an intrinsic depolarized plateau potential, during which neurons are quiescent (Kass & Mintz, 2006). Whatever the underlying mechanism(s), delayed and sustained reductions in activity were seen throughout the rostro-caudal axis of STN. Furthermore, these responses could be evoked by stimulation of either frontal or temporal cortices. Taken together, these findings suggest that the underlying circuits are less strictly organized than the highly topographic corticosubthalamic projections.

The fact that the discharge rates of most STN neurons were significantly reduced for about 200 ms after cortical stimulation indicates that they underwent prolonged membrane hyperpolarization from voltages associated with prestimulation (spontaneous) activity (but see Kass & Mintz, 2006). Although this scheme is corroborated by *in vivo* intracellular data (Kitai & Deniau, 1981), it should be noted that such a hyperpolarization might not be caused by inhibitory synaptic input (Fujimoto & Kita, 1993). Subthalamic nucleus neurons exhibit autonomous oscillatory activity, nonlinear input–output properties, and may express up to four self-sustained membrane states (Bevan & Wilson, 1999; Beurrier *et al.* 2000; Hallworth *et al.* 2003; Kass & Mintz, 2006). Hyperpolarization of the somatodendritic domains of STN neurons can reset the pacemaker oscillation of STN neurons such that, upon repeated stimulation, subsequent discharges appear to be phase-locked to the end of the hyperpolarization (Bevan *et al.* 2000, 2002*a*). Furthermore, prolonged membrane hyperpolarization may be sufficient to de-inactivate low-threshold (T-type) Ca^{2+} channels and/or gait hyperpolarization-activated mixed-cation (I_h) channels, both of which are non-operational during sustained single-spike activity (Beurrier *et al.* 1999; Bevan & Wilson, 1999; Bevan *et al.* 2000, 2002*a*). The cessation of membrane hyperpolarization may be marked by a period of 'rebound activity' that is supported by these channels. Such rebound activity can take the form of rhythmic, single-spike firing or bursting activity, depending on the duration and magnitude of the preceding hyperpolarization (Bevan *et al.* 2000, 2002*a*). Thus, the delayed oscillatory discharges of STN neurons observed in the present study may be a function, at least in part, of the recovery from hyperpolarization and the subsequent resetting of activity. Of particular note in this regard is the possibility that rebound burst activity in STN neurons might constitute either a parallel or supplementary mechanism to the thalamocortical drive that is an important mediator of the delayed cortical response that occurs after the prolonged inhibition evoked by electrical stimulation (Grenier *et al.* 1998). That said, the delayed oscillations could also arise during recovery from a depolarized plateau potential (Kass & Mintz, 2006). It should be remembered, however, that although STN neurons can oscillate in the absence of synaptic inputs *in vitro*, it is likely that the activity of STN neurons *in vivo* is subject to afferent control, at least to some degree. Many globus pallidus neurons will also be active 200–600 ms after cortical stimulation and the ensuing barrage of pallidal inputs may play a role in sculpting the oscillatory discharge of STN neurons (Ryan & Clark, 1991; Nambu *et al.* 2000; Bevan *et al.* 2002*a*,*b*). We also cannot rule out the possibility that the delayed oscillatory activity of STN neurons is driven, at least in part, by renewed excitatory input from, for example, the thalamus, the pedunculopontine tegmental nucleus and/or the cortex (Smith *et al.* 1998; Mena-Segovia *et al.* 2004).

Significance of temporal coupling of STN unit activity to frontal ECoG

Coherence between the discharges of single neurons in STN and the ECoG demonstrates that temporal coupling can occur, irrespective of confounding volume-conducted effects from cortex. The systematic phase differences between some STN and ECoG signals also present a strong argument against volume conduction between these sites, while arguing in favour of a true functional association. In addition, although the firing rates of STN neurons could overlap with the band of coherence (see Fig. 4), there was no linear relation between firing rates and coherence across spectra. Thus, it seems unlikely that the delayed effect of cortical stimulation was merely a resetting of periodic neuronal discharge after a sustained period of reduced firing because this mechanism would not explain why the resultant delayed activity was coherent with ECoG. Could coherence between the ECoG and STN arise without functional coupling of the two signals, if, for example, physiologically independent rhythms were reset or contemporaneously evoked at the cortical and STN levels by cortical stimulation? This too seems unlikely as it would not easily explain why one oscillatory signal (the STN unit discharge) was delayed in onset and it would require persistent amplitude- and phase-locking of the signals for up to 600 ms after cortical stimulation. Instead, the delayed and prolonged nature of the coherence between cortex and STN is highly suggestive of an ongoing functional coupling between these structures that maintains amplitude- and phase-locking over time.

It should be remembered that the present results were derived from responses to low-frequency stimulation of cortex in anaesthetized animals and thus, there is at least a possibility that our data might not be wholly representative of the single neuron and population activities present during behaviour. Nevertheless, the spontaneous activity of STN neurons recorded under urethane anaesthesia is similar to that of STN neurons recorded in the unanaesthetized state (Urbain *et al.* 2000). Furthermore, the short-latency responses and prolonged reductions in firing of STN neurons are not strongly dependent on ongoing brain state (Magill *et al.* 2004*a*) or anaesthetic type (cf. with Kolomiets *et al.* 2001). In the absence of comparative (stimulation) data from unanaesthetized animals however, we cannot rule out the possibility that the urethane anaesthesia used here influenced the delayed oscillatory responses of STN neurons. On the other hand, the significance of our findings is supported by studies suggesting that neurons in cortical areas projecting to the STN exhibit a wide range of synchronous network activity during sensory-motor integration and other complex behaviours that are likely to involve the basal ganglia as a whole (Murthy & Fetz, 1996; MacKay, 1997; Roelfsema *et al.* 1997; Donoghue *et al.* 1998; Brown, 2000; Marsden *et al.* 2000, 2001; Baker *et al.* 2001; Engel & Singer, 2001; Engel *et al.* 2001; Lee, 2003; Buzsáki & Draguhn, 2004). Under physiological conditions, the cortical output precipitated by electrical stimulation might be paralleled by the movement-related corollary discharge from cortex to STN (Kitai & Deniau, 1981; Giuffrida *et al.* 1985; Marsden *et al.* 2001). Rhythmic ECoG responses with frequency components similar to those described here have been observed in humans following stimulation of the motor cortex (Paus *et al.* 2001). Furthermore, long-latency oscillations are not a response feature of cortex that is limited to electrical stimulation. Indeed, such oscillations are known to occur in response to natural sensory inputs (Oldfield & Castro-Alamancos, 2003).

While keeping these caveats in mind, we have shown that the exact pattern of synchronization between population activity in the cortex, as reflected in the ECoG, and single-cell activity in STN depends on the type of cortical input received. For a given stimulated cortical area, the response patterns were similar in the same neuron across trials, and across different neurons recorded in the same half of the STN at different times. This suggests that changes in the temporal coupling of oscillations are a stereotyped and topographically organized response to synchronized cortical outputs. Direct excitatory input to STN from the frontal cortex via the so-called 'hyperdirect' corticosubthalamic pathway (Nambu *et al.* 2002), and the ensuing cycle of excitations and inhibitions, are associated with a delayed, and temporary, periodic discharge of STN neurons. This delayed periodic discharge is coherent with oscillations in the frontal cortex over a wide band from 5 to 30 Hz. In contrast, the oscillatory responses of units in caudal STN, which did not receive cortico-subthalamic input, but which did display the sustained firing reductions, are associated with a delayed and temporary coherence with ECoG activity in the 5–15 Hz band only. Similarly, stimulation of the temporal cortical areas that do not project to STN only resulted in minor coherence with cortex at 5–15 Hz. The fact that the delayed periodic discharge of STN neurons tended to lead oscillations in the frontal cortex suggests that at least some STN neurons may indirectly feed-back to, and thence influence, the synchronized activity of cortical neurons (as indexed by ECoG oscillations) following frontal cortical stimulation. Taken together, the stereotyped and organized modifications in temporal coupling between cortex and STN following synchronized cortical output suggest that these changes may be a mechanistically important feature of the response of the STN to cortical efferent activity.

References

Baker SN, Spinks R, Jackson A & Lemon RN (2001). Synchronization in monkey motor cortex during a precision grip task. I. Task-dependent modulation in single-unit synchrony. *J Neurophysiol* **85**, 869–885.

Bergman H, Feingold A, Nini A, Raz A, Slovin H, Abeles M & Vaadia E (1998). Physiological aspects of information processing in the basal ganglia of normal and parkinsonian primates. *Trends Neurosci* **21**, 32–38.

Berke JD, Okatan M, Skurski J & Eichenbaum HB (2004). Oscillatory entrainment of striatal neurons in freely moving rats. *Neuron* **43**, 883–896.

Beurrier C, Bioulac B & Hammond C (2000). Slowly inactivating sodium current (I(NaP) underlies single-spike activity in rat subthalamic neurons. *J Neurophysiol* **83**, 1951–1957.

Beurrier C, Congar P, Bioulac B & Hammond C (1999). Subthalamic nucleus neurons switch from single-spike activity to burst-firing mode. *J Neurosci* **19**, 599–609.

Bevan MD, Magill PJ, Hallworth NE, Bolam JP & Wilson CJ (2002*a*). Regulation of the timing and pattern of action potential generation in rat subthalamic neurons *in vitro* by GABA-A IPSPs. *J Neurophysiol* **87**, 1348–1362.

Bevan MD, Magill PJ, Terman D, Bolam JP & Wilson CJ (2002*b*). Move to the rhythm: oscillations in the subthalamic nucleus-external globus pallidus network. *Trends Neurosci* **25**, 525–531.

Bevan MD & Wilson CJ (1999). Mechanisms underlying spontaneous oscillation and rhythmic firing in rat subthalamic neurons. *J Neurosci* **19**, 7617–7628.

Bevan MD, Wilson CJ, Bolam JP & Magill PJ (2000). Equilibrium potential of $GABA_A$ current and implications for rebound burst firing in rat subthalamic neurons *in vitro*. *J Neurophysiol* **83**, 3169–3172.

Bolam JP (1992). *Experimental Neuroanatomy: A Practical Approach*. Oxford University Press, Oxford, UK.

Boraud T, Brown P, Goldberg JA, Graybiel AM & Magill PJ (2005). Oscillations in the basal ganglia: the good, the bad and the unexpected. In *The Basal Ganglia VIII*, ed. Bolam JP, Ingham CA & Magill PJ, pp. 3–24. Springer, New York.

Brillinger DR (1981). *Time Series – Data Analysis and Theory*, 2nd edn. Holden Day, San Francisco.

Brown P (2000). Cortical drives to human muscle: the Piper and related rhythms. *Prog Neurobiol* **60**, 97–108.

Brown P (2003). Oscillatory nature of human basal ganglia activity: relationship to the pathophysiology of Parkinson's disease. *Mov Disord* **18**, 357–363.

Brown P, Farmer SF, Halliday DM, Marsden J & Rosenberg JR (1999). Coherent cortical and muscle discharge in cortical myoclonus. *Brain* **122**, 461–472.

Brown P, Oliviero A, Mazzone P, Insola A, Tonali P & Di Lazzaro V (2001). Dopamine dependency of oscillations between subthalamic nucleus and pallidum in Parkinson's disease. *J Neurosci* **21**, 1033–1038.

Buzsáki G & Draguhn A (2004). Neuronal oscillations in cortical networks. *Science* **304**, 1926–1929.

Canteras NS, Shammah-Lagnado SJ, Silva BA & Ricardo JA (1990). Afferent connections of the subthalamic nucleus: a combined retrograde and anterograde horseradish peroxidase study in the rat. *Brain Res* **513**, 43–59.

Cassidy M, Mazzone P, Oliviero A, Insola A, Tonali P, Di Lazarro V & Brown P (2002). Movement-related changes in synchronization in the human basal ganglia. *Brain* **125**, 1235–1246.

Courtemanche R, Fujii N & Graybiel AM (2003). Synchronous, focally modulated beta-band oscillations characterize local field potential activity in the striatum of awake behaving monkeys. *J Neurosci* **23**, 11741–11752.

Donoghue JP & Parham C (1983). Afferent connections of the lateral agranular field of the rat motor cortex. *J Comp Neurol* **217**, 390–404.

Donoghue JP, Sanes JN, Hastopoulos NG & Gaál G (1998). Neural discharge and local field potential oscillations in primate motor cortex during voluntary movements. *J Neurophysiol* **79**, 159–173.

Donoghue JP & Wise SP (1982). The motor cortex of the rat: cytoarchitecture and microstimulation mapping. *J Comp Neurol* **212**, 76–88.

Ellaway PH (1978). Cumulative sum technique and its application to the analysis of peristimulus time histograms. *J Physiol* **45**, 320–304.

Engel AK, Fries P & Singer W (2001). Dynamic predictions: oscillations and synchrony in top-down processing. *Nature Rev Neurosci* **2**, 704–716.

Engel AK & Singer W (2001). Temporal binding and the neural correlates of sensory awareness. *Trends Cog Sci* **5**, 16–25.

Fogelson N, Williams D, Tijssen M, van Bruggen G, Speelman H & Brown P (2006). Different functional loops between cerebral cortex and the subthalamic area in Parkinson's disease. *Cereb Cortex* **16**, 64–75.

Fujimoto K & Kita H (1993). Response characteristics of subthalamic neurons to the stimulation of the sensorimotor cortex in the rat. *Brain Res* **609**, 185–192.

Giuffrida R, Li Volsi G, Maugeri G & Perciavalle V (1985). Influences of pyramidal tract on the subthalamic nucleus in the cat. *Neurosci Lett* **54**, 231–235.

Gotman J (1983). Measurement of small time differences between EEG channels: method and application to epileptic seizure propagation. *Electroencephalogr Clin Neurophysiol* **56**, 501–514.

Grenier F, Timofeev I & Steriade M (1998). Leading role of thalamic over cortical neurons during postinhibitory rebound excitation. *Proc Natl Acad Sci U S A* **95**, 13929–13934.

Halliday DM, Conway BA, Farmer SF & Rosenberg JR (1999). Load-independent contributions from motor-unit synchronization to human physiological tremor. *J Neurophysiol* **82**, 664–675.

Halliday DM, Rosenberg JR, Amjad AM, Breeze P, Conway BA & Farmer SF (1995). A framework for the analysis of mixed time series/point process data – theory and application to the study of physiological tremor, single motor unit discharges and electromyograms. *Prog Biophys Mol Biol* **64**, 237–278.

Hallworth NE, Wilson CJ & Bevan MD (2003). Apamin-sensitive small conductance calcium-activated potassium channels, through their selective coupling to voltage-gated calcium channels, are critical determinants of the precision, pace, and pattern of action potential generation in rat subthalamic nucleus neurons *in vitro*. *J Neurosci* **23**, 7525–7542.

Kass JI & Mintz IM (2006). Silent plateau potentials, rhythmic bursts, and pacemaker firing: Three patterns of activity that coexists in quadristable subthalamic neurons. *Proc Natl Acad Sci U S A* **103**, 183–188.

Kita H (1994). Physiology of two disynaptic pathways from the sensorimotor cortex to the basal ganglia output nuclei. In *The Basal Ganglia IV*, ed. Percheron G, McKenzie JS & Féger J, pp. 263–276. Plenum Press, New York.

Kitai ST & Deniau JM (1981). Cortical inputs to the subthalamus: intracellular analysis. *Brain Res* **214**, 411–415.

Kolomiets BP, Deniau JM, Mailly P, Ménétrey A, Glowinski J & Thierry AM (2001). Segregation and convergence of information flow through the cortico-subthalamic pathways. *J Neurosci* **21**, 5764–5772.

Kühn AA, Williams D, Kupsch A, Limousin P, Hariz M, Schneider GH, Yarrow K & Brown P (2004). Event-related beta desynchronization in human subthalamic nucleus correlates with motor performance. *Brain* **127**, 735–746.

Lee D (2003). Coherent oscillations in neuronal activity of the supplementary motor area during a visuomotor task. *J Neurosci* **23**, 6798–6809.

Levy R, Dostrovsky JO, Lang AE, Sime E, Hutchison WD & Lozano AM (2001). Effects of apomorphine on subthalamic nucleus and globus pallidus internus in patients with Parkinson's disease. *J Neurophysiol* **86**, 249–260.

Levy R, Hutchison WD, Lozano AM & Dostrovsky JO (2000). High-frequency synchronization of neuronal activity in the subthalamic nucleus of parkinsonian patients with limb tremor. *J Neurosci* **20**, 7766–7775.

Levy R, Hutchison WD, Lozano AM & Dostrovsky JO (2002). Synchronized neuronal discharge in the basal ganglia of parkinsonian patients is limited to oscillatory activity. *J Neurosci* **22**, 2855–2861.

MacKay WA (1997). Synchronised neuronal oscillations and their role in motor processes. *Trends Cogn Sci* **1**, 176–183.

Magill PJ, Bolam JP & Bevan MD (2000). Relationship of activity in the subthalamic nucleus-globus pallidus network to cortical electroencephalogram. *J Neurosci* **20**, 820–833.

Magill PJ, Bolam JP & Bevan MD (2001). Dopamine regulates the impact of the cerebral cortex on the subthalamic nucleus-globus pallidus network. *Neuroscience* **106**, 313–330.

Magill PJ, Sharott A, Bevan MD, Brown P & Bolam JP (2004*a*). Synchronous unit activity and local field potentials evoked in the subthalamic nucleus by cortical stimulation. *J Neurophysiol* **92**, 700–714.

Magill PJ, Sharott A, Bolam JP & Brown P (2004*b*). Brain state-dependency of coherent oscillatory activity in the cerebral cortex and basal ganglia of the rat. *J Neurophysiol* **92**, 2122–2136.

Marsden JF, Limousin-Dowsey P, Ashby P, Pollak P & Brown P (2001). Subthalamic nucleus, sensorimotor cortex and muscle interrelationships in Parkinson's disease. *Brain* **124**, 378–388.

Marsden JF, Werhahn KJ, Ashby P, Rothwell J, Noachtar S & Brown P (2000). Organization of cortical activities related to movement in humans. *J Neurosci* **20**, 2307–2314.

Maurice N, Deniau JM, Glowinski J & Thierry AM (1998). Relationships between the prefrontal cortex and the basal ganglia in the rat: physiology of the corticosubthalamic circuits. *J Neurosci* **18**, 9539–9546.

Mena-Segovia J, Bolam JP & Magill PJ (2004). Pedunculopontine nucleus and basal ganglia: distant relatives or part of the same family? *Trends Neurosci* **27**, 585–588.

Murthy VN & Fetz EE (1996). Synchronization of neurons during local field potential oscillations in sensorimotor cortex of awake monkeys. *J Neurophysiol* **76**, 3968–3982.

Nambu A, Tokuno H, Hamada I, Kita H, Imanishi M, Akazawa T, Ikeuchi Y & Hasegawa N (2000). Excitatory cortical inputs to pallidal neurons via the subthalamic nucleus in the monkey. *J Neurophysiol* **84**, 289–300.

Nambu A, Tokuno H & Takada M (2002). Functional significance of the cortico-subthalamo-pallidal 'hyperdirect' pathway. *Neurosci Res* **43**, 111–117.

Oldfield E & Castro-Alamancos MA (2003). Input-specific effects of acetylcholine on sensory and intracortical evoked responses in the 'barrel cortex' *in vivo*. *Neuroscience* **117**, 769–778.

Paus T, Sipila PK & Strafella AP (2001). Synchronisation of neuronal activity in the human primary motor cortex by transcutaneous magnetic stimulation: an EEG study. *J Neurophysiol* **86**, 1983–1990.

Paxinos G & Watson C (1986). *The Rat Brain in Stereotaxic Coordinates*, 2nd edn. Academic Press, Sydney, Australia.

Perkel DH, Gerstein GL & Moore GP (1967). Neuronal spike trains and stochastic point processes II. Simultaneous spike trains. *Biophys J* **7**, 419–440.

Roelfsema PR, Engel AK, König P & Singer W (1997). Visuomotor integration is associated with zero time-lag synchronization among cortical areas. *Nature* **385**, 157–161.

Ryan LJ & Clark KB (1991). The role of the subthalamic nucleus in the response of globus pallidus neurons to stimulation of the prelimbic and agranular frontal cortices in rats. *Exp Brain Res* **86**, 641–651.

Ryan LJ & Clark KB (1992). Alteration of neuronal responses in the subthalamic nucleus following globus pallidus and neostriatal lesions in rats. *Brain Res Bull* **29**, 319–327.

Sharott A, Magill PJ, Bolam JP & Brown P (2005*a*). Directional analysis of coherent oscillatory field potentials in the cerebral cortex and basal ganglia of the rat. *J Physiol* **562**, 951–963.

Sharott A, Magill PJ, Harnack D, Kupsch A, Meissner W & Brown P (2005*b*). Dopamine depletion increases the power and coherence of beta (15–30 Hz) oscillations in the cerebral cortex and subthalamic nucleus of the awake rat. *Eur J Neurosci* **21**, 1413–1422.

Singer W (1999). Neuronal synchrony: a versatile code for the definition of relations? *Neuron* **24**, 49–65.

Smith Y, Bevan MD, Shink E & Bolam JP (1998). Microcircuitry of the direct and indirect pathways of the basal ganglia. *Neuroscience* **86**, 353–387.

Sochurkova D & Rektor I (2003). Event-related desynchronization/synchronization in the putamen. An SEEG case study. *Exp Brain Res* **149**, 401–404.

Urbain N, Gervasoni D, Souliere F, Lobo L, Rentero N, Windels F, Astier B, Savasta M, Fort P, Renaud B, Luppi PH & Chouvet G (2000). Unrelated course of subthalamic nucleus and globus pallidus neuronal activities across vigilance states in the rat. *Eur J Neurosci* **12**, 3361–3374.

Williams D, Kühn A, Kupsch A, Tijssen M, Van Bruggen G, Speelman H, Hotton G, Yarrow K & Brown P (2003). Behavioural cues are associated with modulations of synchronous oscillations in the human subthalamic nucleus. *Brain* **126**, 1975–1985.

Williams D, Tijssen M, Van Bruggen G, Bosch A, Insola A, Di Lazzaro V, Mazzone P, Oliviero A, Quartarone A, Speelman H & Brown P (2002). Dopamine-dependent changes in the functional connectivity between basal ganglia and cerebral cortex in humans. *Brain* **125**, 1558–1569.

Acknowledgements

This work was supported by the Medical Research Council UK and the Brain Research Trust. P. J. Magill held a *Fellowship by Examination* at Magdalen College, Oxford, during this study. We thank B. Micklem *ARPS*, E. Norman and C. Francis for technical assistance.